Exceptional-point-enhanced coupled microcavities for ultrasensitive particle sensing

M. Khanbekyan*
Institute for Physical Research, National Academy of Sciences, Ashtarak, Armenia

(Received 12 March 2023; revised 28 May 2023; accepted 25 July 2023; published 10 August 2023)

This paper proposes and analyzes a theoretical concept of a parity-time ($\mathcal{PT}$) symmetry structure of two coupled microresonators. We propose a particle sensing scheme based on exceptional points (EPs), degeneracy points of non-Hermitian systems, where both eigenvalues and eigenvectors coalesce and where a transition from the exact $\mathcal{PT}$ phase to the broken $\mathcal{PT}$ phase occurs. The abrupt nature of this phase transition is used here for enhanced frequency splitting, based on the spectral response characteristics of the resonator electromagnetic field coupled to a single emitter. The method proposes the usage of a strong coupling of an external emitter to a $\mathcal{PT}$-symmetric resonator structure at and near an EP.

DOI: 10.1103/PhysRevA.108.023710

I. INTRODUCTION

Over the past decades the detection and monitoring of different gases has been on demand, due to growing concerns of the environment and higher healthy standards of living. In particular, gases (including carbon dioxide, carbon monoxide, ammonia, etc.) have been treated as one of the major factors that affect and deteriorate indoor air quality, which could have a subsequent impact on personal health.

Gas sensing is one of the areas of sensing where microcavities can be used [1]. Indeed, a microcavity-based sensor has many advantages, including small size, easy integration and detection of light, real-time sensing capabilities, etc. To realize this kind of sensor a microcavity device can be coated with a chemoresponsive layer specific for the gas of interest. The basic principle of the device is based on an interaction of the target gas molecules with the layer that leads to a change in the refractive index of the layer. Subsequently, the change can be detected by a microcavity. Conventional methods for particle sensing in microcavities include, e.g., detection of a mode frequency shift [2], splitting of a pair of degenerate modes of a whispering-gallery-mode (WGM) resonator [3], and detection of a mode linewidth broadening [4].

The alternative path, which we employ in the present paper, is the usage of optical cavities operating at non-Hermitian spectral degeneracies known as exceptional points (EPs) [5]. The behavior of the physical systems at these critical points, where the eigenvalues and the eigenstates coalesce [6], is of a fundamentally different nature compared to the neighboring points. EPs open pathways for new functionalities and performance, including enhanced sensing possibilities due to a strong system response to perturbations around an EP [7]. The interest in EPs has recently sparked the investigation of a particular family of non-Hermitian systems, a so-called $\mathcal{PT}$-symmetric system. It has been shown that $\mathcal{PT}$-symmetric Hamiltonians, despite being non-Hermitian, can have entirely real eigenvalues [8]. More interestingly, changing parameters of the system of the $\mathcal{PT}$-symmetric Hamiltonian can undergo a phase transition to a spontaneously broken symmetry regime accompanied by a real to complex eigenvalue transition, and the phase transition point exhibits EP singularity.

The usage of EPs for sensing is based on the strong response of an EP degeneracy to a small external perturbation [9]. Conventional degeneracies—so-called diabolic points (DPs)—when subjected to an external perturbation, split in frequency, where the splitting is proportional to the perturbation strength. In contrast, frequency splitting in the case of an EP of order n is proportional to the nth root of the perturbation strength, which is larger than the splitting in the case of a DP for small perturbations. In the domain of $\mathcal{PT}$-symmetric systems, an EP-based sensing enhancement has been explored for systems based on coupled cavities. In particular, a $\mathcal{PT}$-symmetric microcavity system has been used for the sensing of mechanical motion [10], and an enhanced sensitivity of single-particle detection by a system of coupled nanobeam cavities has been shown [11]. However, in many cases the realization of EP-based sensing may be accompanied by noise enhancement, leading to a decrease of the signal-to-noise ratio of the sensor [12,13]. In particular, it is argued that although the presence of an EP leads to an enhancement of the spectral response, it may also amplify the noise by the same or larger factor. Moreover, for the sensitivity of frequency splitting around EPs at quantum scales, the intrinsic quantum noise may dominate, prohibiting amplification of the measured optical signal [14,15]. Nonetheless, very recent experimental results on an electromechanical accelerometer show a particular EP-based $\mathcal{PT}$-symmetric system, where the noise can be surpassed by an enhanced signal response, thus revealing the merit of using EPs for sensing [16].

In practice, EPs and related effects are easily accessible with the usage of resonators, which have been investigated as a sample system to study the effects related to wanted and unwanted losses [17]. With respect to the study of light-matter interaction in cavities, it has been shown that the spontaneous emission of dipole emitters in the weak-coupling regime can

*khanbekyan@gmail.com

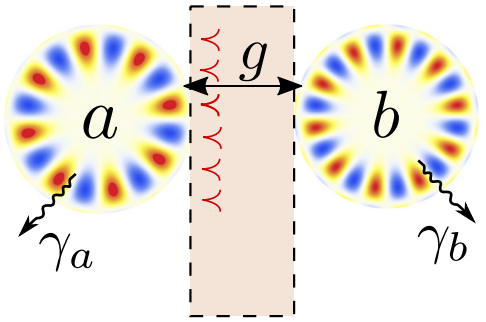

FIG. 1. Schematic graph of the model sensing apparatus. The coupled resonators a and b are illustrated as WGM resonators, where the coupling rate is determined by the distance between them. At the same time, the coupling layer acts as a channel to load analytes, which couple to the resonator a due to the functionalized surface of the resonator.

be modified at an EP, leading to a strong enhancement of the emission rate [18]. The spontaneous emission rate enhancement of an emitter coupled to the resonator at an EP is related to the linear response of a resonant system, which at an EP exhibits a square Lorentzian line shape in contrast to a Lorentzian function in the single-mode case. However, as we have shown recently [19], Rabi splitting of the strong-coupling rate of a single emitter coupled to an EP mode approximately equals the one in the case of a single-mode case, which is smaller than the Rabi splitting in the case of a two-mode cavity. Moreover, the interaction of a single emitter with a WGM resonator at an EP provides a strong spectroscopic tool for the sensitive enantioselection of chiral molecules [20].

In the ensuing paper, we present a gas sensing structure, where we propose to use coupling of an external emitter with a microcavity system at and near the EP regime. In contrast to our previous works [19,20], here, the platform is based on a system of coupled resonators, that obeys $\mathcal{PT}$ symmetry and that possesses an EP (see Fig. 1). Provided the system is prepared in the EP state and that target molecules couple to the surface of one of the resonators, a perturbation to the system is imposed, which leads the system away from the EP. This way, the emission of an emitter coupled to the resonator provides the spectral signature of the perturbation, since as the perturbation increases, the Rabi splitting of strong emitter-field coupling increases in comparison to the EP case.

II. COUPLED CAVITIES IN A $\mathcal{PT}$-SYMMETRIC CONFIGURATION

We study the simplest system, composed of two coupled resonators, by means of coupled-mode theory [21]. For the realization of an EP the required key feature is that the modes of the non-Hermitian system possess the same frequency but different loss rates. The frequencies and the loss rates of modes are defined by means of the real and imaginary parts of the mode eigenfrequencies, correspondingly. In a particular case of a coupled system with balanced loss and gain, a $\mathcal{PT}$-symmetric EP can be achieved.

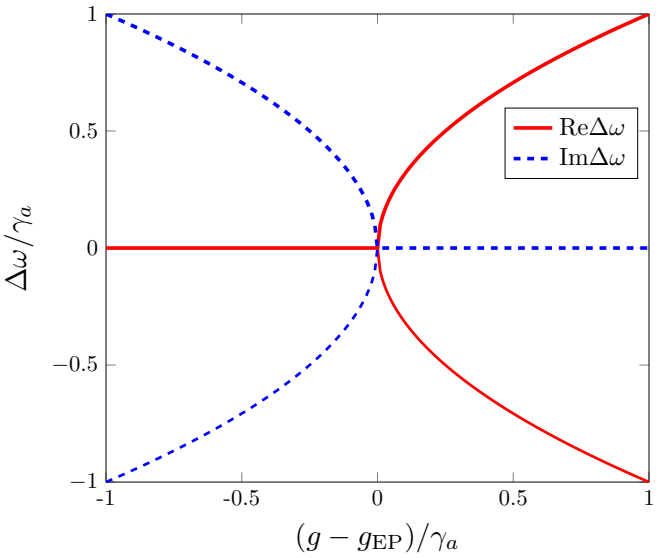

FIG. 2. Real (red, solid) and imaginary (blue, dashed) parts of $\Delta\omega$ with respect to the coupling strength.

Starting with the coupled-mode theory for two coupled microcavities, the time evolution of the system can be described by a Schrödinger-type equation in a two-mode approximation on the basis of two cavity modes [22],

$$i\frac{d}{dt}\boldsymbol{\psi} = \mathcal{H}\boldsymbol{\psi}, \tag{1}$$

with the effective Hamiltonian (see Ref. [6])

$$\mathcal{H} = \begin{pmatrix} \omega_a - i\gamma_a/2 & g \\ g & \omega_b - i\gamma_b/2 \end{pmatrix}, \tag{2}$$

where (real) g is the coupling rate between the modes of the resonators, and $\omega_{a,b}$ are the mode frequencies. In the following, we consider a quasi-$\mathcal{PT}$-symmetric case, where both γ_a and γ_b describe (nonequal, $\gamma_a \neq \gamma_b$) loss rates of the a and b resonators, correspondingly. If $\omega_a = \omega_b \equiv \omega_0$, the two eigenvalues associated with this Hamiltonian read as follows:

$$\lambda_\pm = \omega_0 - i(\gamma_a + \gamma_b)/4 \pm \sqrt{g^2 - (\gamma_a - \gamma_b)^2/16}. \tag{3}$$

From Eq. (3) it can be seen that in the case of large coupling strengths, $g > |\gamma_a - \gamma_b|/4$, the square-root term on the right-hand side of Eq. (2) is real, and the system resides in the regime for which the coherent energy exchange between two resonators compensates for the decay difference, and both modes have the same decay rate $(\gamma_a + \gamma_b)/4$, corresponding to the $\mathcal{PT}$-symmetric phase. If the coupling is small, $g < |\gamma_a - \gamma_b|/4$, the square-root term is imaginary, and the system possesses two modes with different decay rates, which corresponds to the $\mathcal{PT}$-symmetry broken phase.

The EP point emerges at $g = g_{\rm EP} \equiv |\gamma_a - \gamma_b|/4$, that manifests itself as a critical point between the two phases [23] (see Fig. 2). In this case, the eigenfrequencies coalesce at $\lambda_{\rm EP} = \omega_0 - i(\gamma_a + \gamma_b)/4$, and the remaining (right) eigenstate reads

$$\boldsymbol{\psi}^{\rm R}_{\rm EP} = \frac{1}{4}\begin{pmatrix} i(\gamma_b - \gamma_a) \\ |\gamma_b - \gamma_a| \end{pmatrix}, \tag{4}$$

which, together with the left eigenvector $(\boldsymbol{\psi}_{\rm EP}^{\rm L})^{\rm T} = (1/4)(|\gamma_a - \gamma_b|\ i(\gamma_a - \gamma_b))$, satisfies the self-orthogonality condition $(\boldsymbol{\psi}_{\rm EP}^{\rm L})^{\rm T} \cdot \boldsymbol{\psi}_{\rm EP}^{\rm R} = 0$, where the superscript T denotes the transpose [6]. Note that the losses of the passive system under consideration are always present both in the $\mathcal{PT}$-symmetric phase and in the EP case, where $g = |\gamma_a - \gamma_b|/4$ can still be positive for different loss rates γ_a and γ_b.

The spectral response of the system is characterized by the Green tensor which, near the EP, can be found using the Jordan chain relation as [19,20]

$$\boldsymbol{G}_{\rm EP}(\omega) = \frac{1}{4}\frac{1}{(\omega - \lambda_{\rm EP})^2}\begin{pmatrix} i(\gamma_b - \gamma_a) & |\gamma_a - \gamma_b| \\ |\gamma_b - \gamma_a| & i(\gamma_a - \gamma_b) \end{pmatrix} + \frac{1}{\omega - \lambda_{\rm EP}}\begin{pmatrix} 1 & 0 \\ 0 & 1 \end{pmatrix}, \tag{5}$$

which yields the expansion of the Green tensor into the a and b resonator mode functions as

$$\begin{aligned} \mathsf{G}_{\rm EP}(\mathbf{r}, \mathbf{r}', \omega) = {} & \frac{1}{4}\frac{1}{(\omega - \lambda_{\rm EP})^2} \\ & \{i(\gamma_b - \gamma_a)[\boldsymbol{E}_a(\mathbf{r})\boldsymbol{E}_a(\mathbf{r}') - \boldsymbol{E}_b(\mathbf{r})\boldsymbol{E}_b(\mathbf{r}')] \\ & + |\gamma_b - \gamma_a|[\boldsymbol{E}_a(\mathbf{r})\boldsymbol{E}_b(\mathbf{r}') + \boldsymbol{E}_b(\mathbf{r})\boldsymbol{E}_a(\mathbf{r}')]\} \\ & + \frac{1}{\omega - \lambda_{\rm EP}}[\boldsymbol{E}_a(\mathbf{r})\boldsymbol{E}_a(\mathbf{r}') + \boldsymbol{E}_b(\mathbf{r})\boldsymbol{E}_b(\mathbf{r}')]. \end{aligned} \tag{6}$$

A remarkable feature of this Green tensor is the presence of the second-order pole that appears at the EP. Note that, in the case $\gamma_a = \gamma_b$, and therefore $g_{\rm EP} = 0$, the system governed by the Hamiltonian Eq. (2) features a conventional degeneracy (a diabolic point) at which the second-order pole of the Green tensor [the first term in Eq. (6)] vanishes.

Our approach is based on the peculiar spectral response of the electromagnetic field at the EP [19]. Thus, we study radiative emission of a single emitter (position $\mathbf{r}_A$) interacting with the electromagnetic field in the dipole approximation [24],

$$\hat{H}_{\rm int} = -\hat{\mathbf{d}} \cdot \hat{\mathbf{E}}(\mathbf{r}_A), \tag{7}$$

which contains the electric dipole-moment operator of the emitter, that can be represented by means of the flip operators as

$$\hat{\mathbf{d}} = \sum_{mn} \mathbf{d}_{mn}\hat{S}_{mn}, \tag{8}$$

with $\mathbf{d}_{mn} = \langle m|\hat{\mathbf{d}}|n\rangle$, and $\hat{S}_{mn}$ being the flip operators,

$$\hat{S}_{mn} = |m\rangle\langle n|. \tag{9}$$

Let us assume that only a single transition ($|1\rangle \leftrightarrow |2\rangle$, frequency ω_{21}, dipole moment $\mathbf{d}_{21}$) is quasiresonantly coupled to a narrowband cavity-assisted electromagnetic field, and that the emitter is initially (at time $t = 0$) prepared in the excited state $|2\rangle$, and the field of the resonators is in its ground state $|\{0\}\rangle$. Then, restricting the system to single excitations, the Schrödinger equation reduces to the following integrodifferential equation for the excited-state amplitude $C_2(t)$ (for details, see Ref. [25]):

$$\dot{C}_2(t) = \int_0^t dt'\, K(t - t')C_2(t'). \tag{10}$$

In the above, the kernel function $K(t)$ reads

$$K(t) = -\frac{1}{\pi\hbar\varepsilon_0}\int_0^\infty d\omega \frac{\omega^2}{c^2} e^{-i(\omega-\omega_{21})t} \times \mathbf{d}_{21} \cdot {\rm Im}\,\mathsf{G}(\mathbf{r}_A, \mathbf{r}_A, \omega) \cdot \mathbf{d}_{21}^*. \tag{11}$$

In the following, we focus on a situation when the emitter couples only to the a mode, with $\mathbf{d}_{21} \cdot \boldsymbol{E}_b(\mathbf{r}) = 0$. Then, using the expression for the Green tensor of the coupled microresonator system at the EP, Eq. (6), we can solve the integrodifferential equation, Eq. (10), together with Eq. (11). The solution for the excited-state probability $|C_2(t)|^2$ shows Rabi oscillations [see Fig. 3(a)] that reflect the strong-coupling regime between the emitter and the field (for details, see Ref. [26]). In addition, as Fig. 3(b) reveals, the strong-coupling regime is characterized by the Rabi splitting R of the spectral mode function of the outgoing field.

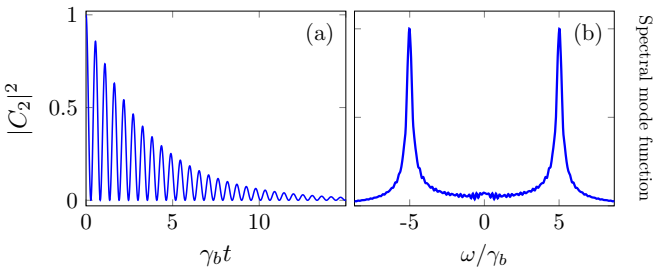

FIG. 3. (a) Excited-state amplitude $|C_2(t)|^2$, and (b) spectral mode function of the outgoing field at EP for $\gamma_p = -\gamma_a/2$, $\omega_{21} = \omega_0 = 10^5\gamma_a$ at an emitter-field coupling rate of $r = 10\gamma_a$.

To illustrate how the proposed system can be used for sensing applications, let us now suppose that we introduce a small perturbation to the system, which disturbs the EP. Namely, we assume that the coupling rate between the two resonators slightly changes $g = g_{\rm EP} + v$, where v is the small perturbation. In this case, the eigenvalues of the system read

$$\lambda_\pm = \omega_0 - i(\gamma_a + \gamma_b)/4 \pm \sqrt{v}, \tag{12}$$

which reveals that when $v < 0$, which corresponds to reduction of the coupling rate in comparison to the EP rate, $g < g_{\rm EP}$, the perturbation introduces a small change to the decay rates of the resonators. In contrast, when $v > 0$, i.e., $g > g_{\rm EP}$, the perturbation changes the real parts of the eigenvalues. Therefore, in this case the system transforms from the regime of the EP to the regime of the two-mode case, where increasing the perturbation v increases the detuning of the resonant frequency (details of the calculation of a single-emitter coupling to two modes can be found in Ref. [26]). Then, the Rabi splitting R, which now corresponds to the strong coupling of the emitter to the two modes (resonators), increases in comparison to the Rabi splitting of the single EP-mode case $R_{\rm EP}$ (see Fig. 4).

To illustrate the advantages of the EP-based sensing in comparison to the conventional DP-based sensing, in the inset of Fig. 4 we present a comparison of the Rabi splitting for

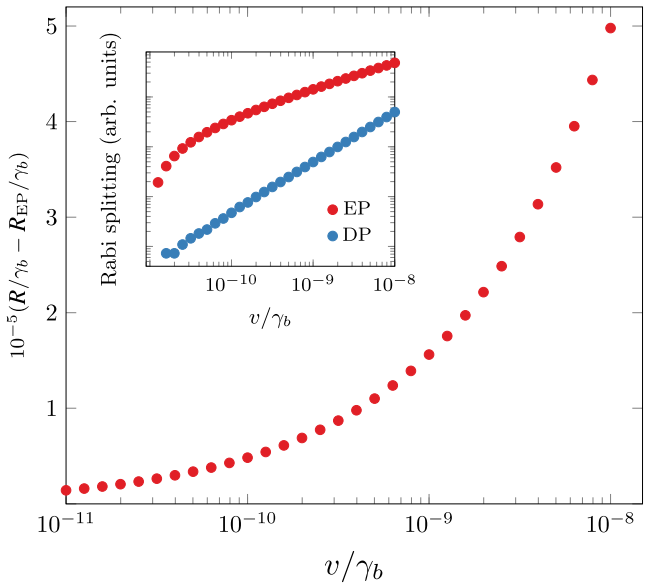

FIG. 4. Dependence of the Rabi splitting R on the perturbation of the coupling rate v. Inset: Comparison of the Rabi splitting for the EP case and DP case in a log-log plot. Parameter values are the same as in the Fig. 3.

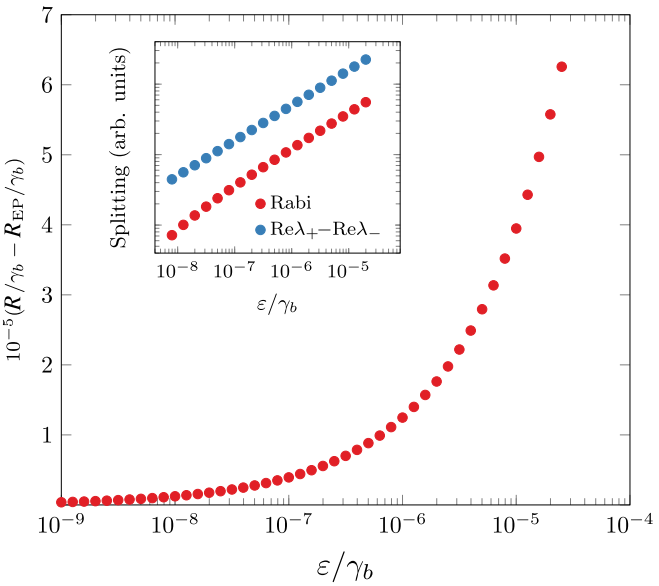

FIG. 6. Dependence of the Rabi splitting R on the perturbation ε. In the inset we present a comparison of Rabi splitting in the strong-coupling regime with eigenvalue splitting of the passive system in a log-log scale. Parameter values are the same as in Fig. 3.

the two cases. A diabolic point can be obtained when we put $g = 0$ and $\gamma_a = \gamma_b$ in Eq. (2). The inset of Fig. 4 confirms the enhanced frequency splitting of the EP case in comparison to the DP case.

III. SENSING MECHANISM FOR PARTICLE DETECTION

The sensor is based on a quasi-$\mathcal{PT}$-symmetric coupled resonator system, where the coupling layer represents a channel for the load of the gas sample. The surface of the cavity a binds specific target gas molecules. When a particle is bonded to the surface of the resonator a, the perturbation of strength ε is introduced, which increases the absorption of the first cavity. As Fig. 5 reveals, increasing absorption ($\varepsilon > 0$) brings the system from the EP to the unbroken $\mathcal{PT}$-symmetry state, where the real parts of eigenfrequencies split, but the imaginary parts remain equal. In this way, the system of coupled resonators undergoes a transition from the single EP-mode state to the two-mode state. Stronger absorption leads to an increase in the splitting of the real parts of the mode eigenvalues.

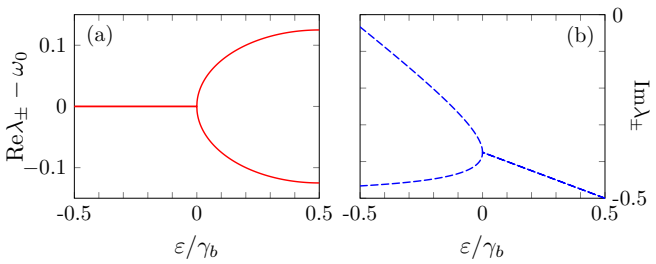

FIG. 5. (a) Real and (b) imaginary parts of eigenvalues with respect to the perturbation strength ε for $g/\gamma_b = 0.125$, and $\gamma_a/\gamma_b = 0.5$.

In order to see how the presence of a scatterer modifies the spectral response of the resonator system, we study the radiative emission of a single emitter coupled to the first cavity. From Fig. 6 we can see that the Rabi splitting of the strong emitter-field coupling R increases as the resonator system switches from the EP regime to the double-mode regime. In the inset of Fig. 6 we compare the splitting of a conventional passive $\mathcal{PT}$-symmetric sensing, where the splitting of eigenfrequencies is detected. As the figure reveals, although the eigenfrequency splitting is slightly larger than the Rabi splitting, both splittings are of the same order of magnitude and show a square-root dependence on the perturbation strength.

IV. CONCLUSIONS

In summary, we have presented a method for biosensing based on the interaction of a single emitter with a system of coupled resonators in a $\mathcal{PT}$-symmetric configuration. The method utilizes the spectral response of coupled cavities operating at an EP and the spontaneous emission of the emitter in the strong-coupling regime. In particular, by introducing a perturbation, which represents the presence of the target molecules, the system leaves the EP state into the $\mathcal{PT}$-symmetric state, providing a spectral modification of emission. In this way, the method provides enhanced frequency splitting even for small perturbations, which corresponds to a low concentration of particles to be detected. It should be emphasized that the passive system of coupled resonators has no gain, and $\mathcal{PT}$ symmetry is realized by introducing different loss rates of the resonators. Therefore, a dynamical noise-induced parametric instability of the system characteristic for conventional $\mathcal{PT}$-symmetric gain-loss systems is avoided [27]. At the same time, the present method suggests the usage of spontaneous emission of an external emitter in the strong-coupling regime, which allows us to

avoid a well-known limitation of conventional EP-based lossy sensors—reduction of the resolvability of the frequency splitting due to linewidth broadening. Thus, our study offers an EP-based enhanced frequency splitting, where strong coupling with an external emitter is used. The scheme may offer a feasible sensing method for particle detection with a high sensibility provided an enhanced signal-to-noise ratio is achieved.

ACKNOWLEDGMENT

The author gratefully acknowledges helpful discussions with J. Wiersig. This research was done in the frame of the Faculty Research Funding Program implemented by the Enterprise Incubator Foundation (EIF), with the support of PMI Science.

[1] X. Jiang, A. J. Qavi, S. H. Huang, and L. Yang, Matter **3**, 371 (2020).
[2] F. Vollmer, S. Arnold, and D. Keng, Proc. Natl. Acad. Sci. USA **105**, 20701 (2008).
[3] J. Zhu, S. K. Ozdemir, Y.-F. Xiao, L. Li, L. He, D.-R. Chen, and L. Yang, Nat. Photon. **4**, 46 (2010).
[4] B.-Q. Shen, X.-C. Yu, Y. Zhi, L. Wang, D. Kim, Q. Gong, and Y.-F. Xiao, Phys. Rev. Appl. **5**, 024011 (2016).
[5] M.-A. Miri and A. Alù, Science **363**, eaar7709 (2019).
[6] W. Heiss, J. Phys. A: Math. Theor. **45**, 444016 (2012).
[7] H. Hodaei, A. U. Hassan, S. Wittek, H. Garcia-Gracia, R. El-Ganainy, D. N. Christodoulides, and M. Khajavikhan, Nature (London) **548**, 187 (2017).
[8] C. M. Bender and S. Boettcher, Phys. Rev. Lett. **80**, 5243 (1998).
[9] J. Wiersig, Photon. Res. **8**, 1457 (2020).
[10] Z.-P. Liu, J. Zhang, Ş. K. Özdemir, B. Peng, H. Jing, X.-Y. Lü, C.-W. Li, L. Yang, F. Nori, and Y.-X. Liu, Phys. Rev. Lett. **117**, 110802 (2016).
[11] S. Zhang, Z. Yong, Y. Zhang, and S. He, Sci. Rep. **6**, 24487 (2016).
[12] H.-K. Lau and A. A. Clerk, Nat. Commun. **9**, 4320 (2018).
[13] J. Wiersig, Nat. Commun. **11**, 2454 (2020).
[14] R. Duggan, S. A. Mann, and A. Alù, ACS Photon. **9**, 1554 (2022).
[15] D. Anderson, M. Shah, and L. Fan, Phys. Rev. Appl. **19**, 034059 (2023).
[16] R. Kononchuk, J. Cai, F. Ellis, R. Thevamaran, and T. Kottos, Nature (London) **607**, 697 (2022).
[17] A. A. Semenov, D. Y. Vasylyev, W. Vogel, M. Khanbekyan, and D.-G. Welsch, Phys. Rev. A **74**, 033803 (2006).
[18] A. Pick, B. Zhen, O. D. Miller, C. W. Hsu, F. Hernandez, A. W. Rodriguez, M. Soljačić, and S. G. Johnson, Opt. Express **25**, 12325 (2017).
[19] M. Khanbekyan and J. Wiersig, Phys. Rev. Res. **2**, 023375 (2020).
[20] M. Khanbekyan and S. Scheel, Phys. Rev. A **105**, 053711 (2022).
[21] W. Chen, Ş. K. Özdemir, G. Zhao, J. Wiersig, and L. Yang, Nature (London) **548**, 192 (2017).
[22] I. Rotter, J. Phys. A: Math. Theor. **42**, 153001 (2009).
[23] C. E. Rüter, K. G. Makris, R. El-Ganainy, D. N. Christodoulides, M. Segev, and D. Kip, Nat. Phys. **6**, 192 (2010).
[24] W. Vogel and D.-G. Welsch, *Quantum Optics*, 3rd ed. (Wiley-VCH, Weinheim, 2006).
[25] M. Khanbekyan, D.-G. Welsch, C. Di Fidio, and W. Vogel, Phys. Rev. A **78**, 013822 (2008).
[26] M. Khanbekyan, Phys. Rev. A **97**, 023809 (2018).
[27] J. Wiersig, Phys. Rev. A **101**, 053846 (2020).